Biointerface Research in Applied Chemistry
Platinum Open Access Journal (ISSN: 2069-5837)

Article
Volume 11, Issue 4, 2021, 11653 - 11665
https://doi.org/10.33263/BRIAC114.1165311665

Preparation of Chitosan/Hyperbranched Polyester/Cobalt Composite For Acid Blue 277 Dye Adsorption

Ahmed A. Haroun [1,*], Fatma Abdelghaffar [2], Osama A. Hakeim [2]

[1] Chemical Industries Research Division, National Research Center, Dokki, Cairo, Egypt
[2] Textile Research Division, National Research Center, Dokki, Cairo, Egypt
* Correspondence: haroun68_2000@yahoo.com;

Scopus Author ID 7003267177

Received: 18.11.2020; Revised: 11.12.2020; Accepted: 13.12.2020; Published: 16.12.2020

Abstract: Acid dye effluents are among the popular threatening sources to the environment and human health due to their photochemical stability, complexity, and poor biodegradability. Therefore, this study aims to prepare chitosan/hyperbranched polyester (HBPE)/cobalt composite with ratio (1:1:0.5 wt %, respectively) using emulsion technique as an adsorbent to deal with the acid dye effluent. Chemical structure, morphology, particle size analysis, and thermal stability of the prepared composite were carried out using Fourier transform infrared spectroscopy (FTIR), scanning electron microscope (SEM),) dynamic light scattering technique (DLS) and thermogravimetric analysis (TGA). Adsorption isotherms of acid blue 277 dye (AB277), using the different isotherm models (Langmuir, Freundlich, D-R, and Temkin) under removal conditions at pH 3.0 and contact time of 1 h in 10 mL aqueous medium at 25^{O}C, were investigated. The results illustrated that the chitosan/HBPE/Co composite was successfully prepared with a particle size of around 679±494 nm relative to chitosan/HBPE (139±67.6 nm). Also, the pseudo-second-order kinetic model fitted better than the pseudo-first-order one for adsorption of AB277. Batch equilibrium studies showed that chitosan/HBPE/Co composite could be employed as an efficient adsorbent of AB277 dye with an adsorption capacity of 26.74 mg/g, relative to that of chitosan/HBPE (3.19 mg/g).

Keywords: chitosan; hyperbranched polyester; dye effluent; acid blue 227 dye; adsorption kinetics; Isotherm models.

1. Introduction

The main objective of this work deals with using carbohydrate polymer (chitosan) as a support material for the preparation of adsorbents of the toxic materials, where there is no specific involvement of the chemistry of the carbohydrate polymer hyperbranched polyesters. It's important to discover the adsorption isotherms and the kinetics study of newly adsorbents based on modified chitosan for environmental application. Toxic and hazardous substances, colors, and pigments are sources of contamination, which is a dangerous problem and is expected to increase in the years ahead [1-3]. Printing, fiber, paper, electroplating, cosmetics, pharmaceuticals, and food industries effluents are the primary causes of water pollution. The technologies for removing dye from aquatic environments have been enhanced, including chemical, physical, and even biological techniques. Several adsorbent products are used in the water purification process, such as newspaper waste, thermoplastics, polystyrene waste, gelatin/chitosan composites, and wool fibers, clays, biopolymers, polysaccharides (modified chitosan) and activated carbon, etc. [4-37]. Chitosan is a biopolymer obtained from partial or

complete deacetylation of chitin, a copolymer of N-acetyl-dglucosamine and D-glucosamine units linked by (1-4) glycosidic bonds, where N-acetyl-D-glucosamine units predominate in the biopolymer chain [38, 39]. The main advantage of chitosan concerning the preparation of new derivatives relative to cellulose is the presence of a primary amine group at the pyranosidic ring position C-2. This amine group makes it possible to prepare different new materials with new chemical properties, using different synthesis strategies for new applications [40]. One of these applications is as an adsorbent material for removing heavy metal ions and dyes from water and wastewater in cationic and/or anionic forms. However, Chitosan is known to be highly prone to pH changes, as it can either form a gel or dissolve. Therefore, the chemical modifications of chitosan should always consider the improvement of its properties, such as solubility and swelling. Previously, the ability of chitosan and chitosan-EGDE (ethylene glycol diglycidyl ether) beads to extract acid red 37 (AR37) and acid blue 25 (AB25) from an aqueous solution was examined [41]. Modeling experimental isothermic adsorption data is an essential way to predict and compare adsorption mechanisms critical to optimizing adsorption pathways, expressing adsorbent capacities, and effectively designing adsorption systems [42]. Several isothermic two-parameter models are commonly used to model the adsorption data, such as Langmuir, Freundlich, D-R, and Temkin [43-46]. This paper used four isotherm models, namely: Langmuir, Freundlich, Dubinin-Radushkevich (D-R), and Temkin, to compare four sets of isothermic experimental adsorption results, which were obtained through batch testing in the laboratory. This study also reports the preparation of chitosan/hyperbranched polyester (HBPE) composite in the presence of cobalt acetate as an efficient material using the emulsion technique for environmental remediation. Various analyzes have been used to describe and investigate such materials as FTIR, SEM, particle size distribution, and TGA. Both products have been used and measured as possible sorbents for removing AB277 dye from aqueous solution. It examined the impact of temperature, pH, dye concentration, and contact time on the adsorption procedure. Also, the adsorption isotherm data for removing AB277 from a novel adsorption system (chitosan/HBPE/Co) were modeled using a linearized method. The parameters' predictive accuracy for the various isotherm models was compared and discussed to establish the most appropriate correlation of the adsorption equilibrium. Modeling results are expected to provide some theoretical basis for the operational design and practical application of color removal adsorption systems, which has attracted growing interest in water protection.

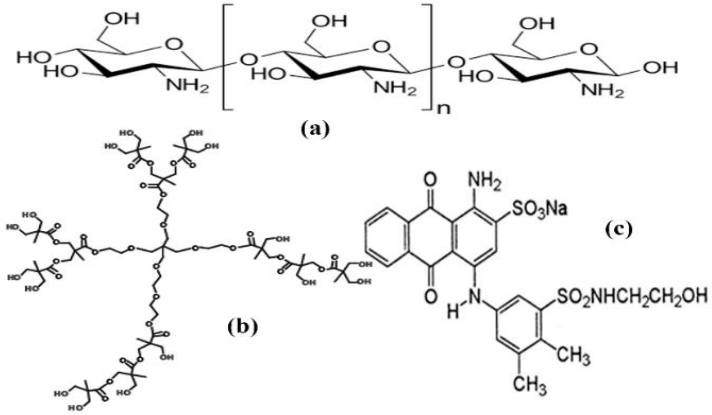

Figure 1. Chemical structures of (a) chitosan, (b) HBPE, and (c) AB277.

2. Materials and Methods

2.1. Materials.

Hyperbranched bis-MPA polyester-16-hydroxyl, generation 2 (HBPE-16), ≥97%, CAS No: 326794-48-3, Mol Wt: 1749.79 and chitosan low molecular weight, CAS No: 9012-76-4, Mol Wt: 50,000-190,000 Da (based on viscosity) and 75-85% deacetylated, were supplied by Sigma-Aldrich, Germany. C.I. Acid blue 277, 98%, obtained from Ciba, Egypt. (The chemical structures were illustrated in Figure 1). All other chemicals and reagents were used as received.

2.2. Methods.

2.2.1. Preparation of chitosan/HBPE using emulsion technique.

After homogenization with high-speed sonification, emulsion experiments were performed in tubes. In the presence of cobalt acetate (0.5 mg), chitosan (10 mg) was dissolved in the aqueous acidic medium. The solution was mixed with HBPE-16 at wt ratio 1:1 in an aqueous solution with a definite quantity of cetyl trimethyl ammonium bromide (CTAB) in the ultrasonic process (3 min at 200 W). The same ingredients were prepared without cobalt salt in another experiment. Separated the resulting materials using a centrifuge, then gathered and held for further examination [47].

2.2.2. Characterization.

All the prepared materials were characterized using different analytical tools: Perkin-Elmer Fourier transform infrared spectroscopy (FTIR) under certain condition such as: scan resolution: 4 cm^{-1}, scan rate: 2 mm/sec, number of scan: 32, range: 600- 3800 cm^{-1} and mode: transmission. The shapes and morphologies of the preparations were examined by scanning electron microscopy using JEOL-SEM, Japan. The particle size distribution analysis was recorded at run time: 2 min, temperature: 23˚C, solvent: water, concentration: 1 mg/mL, using Gaussian/Nicomp distribution analysis, particle sizing systems Inc. Santa Barbara, California, USA. Thermogravimetric analysis (TGA) of the prepared samples was carried out on Perkin- Elmer thermogravimetric analyzer TGA 7. The dry samples were heated from room temperature to 700°C at 5°C/min.

2.2.3. Batch adsorption experiments.

Adsorption experiments were conducted in a batch method *via* suspending 0.05 g of the prepared materials (chitosan/HBPE or chitosan/HBPE/Co) was mixed with 10 mL of AB277 dye solution (46.59 mg/L) at pH 3 in an Erlenmeyer flask. The mixture was equilibrated on a water shaker thermostat for 1 h at 60 rpm and 25±0.2°C. The adsorption of AB277 onto chitosan/HBPE or chitosan/HBPE/Co was studied at initial dye concentrations (46.59-207.39 mg/L) and temperature range (40 and 60±0.2°C). The samples were separated using (Centrifuge-Sigma). The adsorbate's residual concentrations were measured by recording the absorbance of the supernatant at λmax 630 nm using a UV/Vis Spectrometer Shimadzu, Japan. The adsorption isotherms and kinetics were analyzed *by* determining the adsorption capacities at various time intervals. The adsorption capacity (q_e), was calculated by Eq. (1):

$$Q_e = (C_0-C_e)\ V/m \qquad (1)$$

Where C_0 and C_e are representatives of the initial and equilibrium concentrations, AB277 was used. Moreover, V is the volume (mL) of MG solution, and m is the mass (g) of the chitosan/HBPE or chitosan/HBPE/Co. All the mean values have been reported.

2.2.3.1. Sorption isotherms of AB 277.

The AB 277 dye filtrates were analyzed and fitted into the following adsorption isotherms [48]: Langmuir, Freundlich, Dubinin-Raduskevich (D-R) and Temkin

2.2.3.2. Kinetic studies.

Adsorption kinetics models can be used to simulate the uptake of AB 277 by adsorbents. To investigate the adsorption kinetics of AB 277 onto the adsorbents, two well–known kinetic models, i.e., the pseudo-first-order and the pseudo-second-order models, are implemented [49]. The rate constants of AB277 adsorption are determined from the following Equations:

$$\log (Q_e - Q_t) = \log Q_e - (K_1/2.303)\, t \quad (2)$$

$$t/Q_t = [1/K_2 (Q_e)^2] + (1/Q_e)\, t \quad (3)$$

Where, Q_e and Q_t are the amounts of AB 277 adsorbed (mol/g) at equilibrium and after contact time t (min) of adsorption, respectively. K_1 and K_2 are the pseudo-first and pseudo-second-order rate constants, respectively.

3. Results and Discussion

3.1. Characterization of the prepared composites.

Figure 2 shows FTIR spectra of the prepared composites (chitosan/HBPE/Co and chitosan/HBPE) in comparison with chitosan. The main bands appearing in the spectrum of chitosan were due to axial stretching vibration of O-H superimposed on the N-H stretching band and the interhydrogen bonds of the polysaccharide in the range 3700-3400 cm^{-1} and the C-H bond in the $–CH_2$ 2840 cm^{-1} and $–CH_3$ 2903 cm^{-1} groups. The other bands observed in the vibration spectrum of chitosan were –C=O stretching of the amide group coupled with N-H bending 1604-1592 cm^{-1}, C-N stretching coupled with N-H plane deformation 1402 cm^{-1}, C-O-C bridge stretching vibration 1074 $cm^{-1,}$ and the specific bands of the β-(1-4) glycoside bridge 1133 and 819 cm^{-1}. It was anticipated that coordination of the nitrogen center with the metal ion (Co) would reduce the electron density in the amino group and shifts the frequencies of N-H stretching and plane bending to lower wavenumbers, indicating successful coordination of this amino nitrogen with the metal center [50, 51].

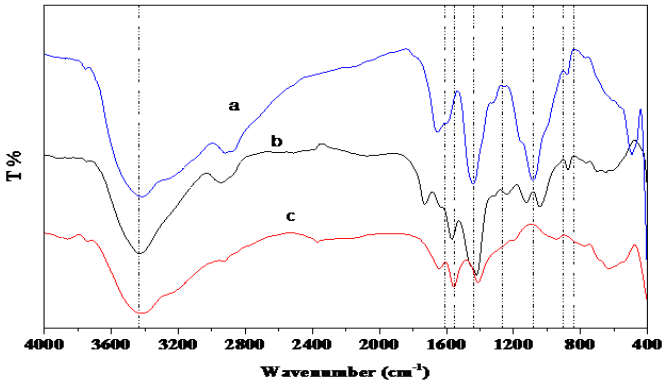

Figure 2. FTIR spectra of (a) Chitosan, (b) Chitosan/HBPE, and (c) Chitosan/HBPE/Co.

Figure 3 presents the SEM-micrographs of the prepared composites. Co metals (shiny white form) had agglomerated, as can be seen, on the surface and inside the chitosan/HBPE composite structure. The composite surface of chitosan/HBPE, though, had a broad porosity structure. Then again, on account of chitosan/HBPE/Co and chitosan/HBPE composites, the molecule size conveyance investigation utilizing the DLS system indicated breadths of about 679±494 and 139±67.6 nm, separately. It tends to be inferred that the normal width size within sight of Co metal particles was bigger because of SEM, which could be because of fractional agglomeration and expansion in water. Those outcomes demonstrated a decent interchange between the network of chitosan and HBPE. The chitosan-progress metal mixes' warm properties were beforehand studied by TGA under nitrogen air [52]. All in all, it has been discovered that the coordination of a metal particle with the useful gathering of the chitosan moiety causes warm flimsiness and influences warm corruption.

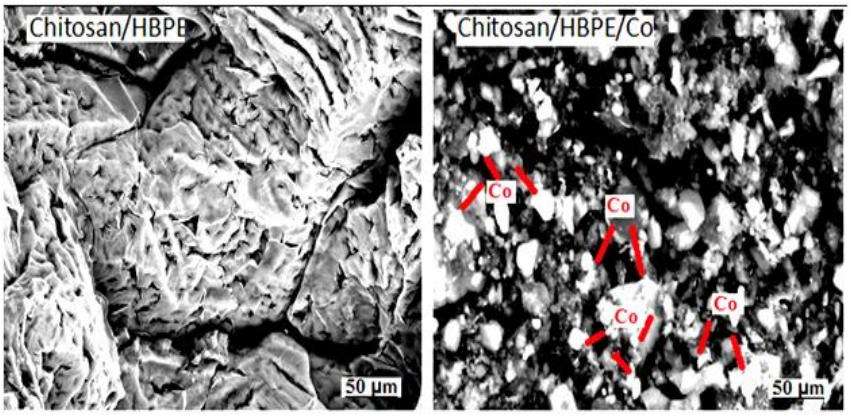

Figure 3. SEM-micrographs of the prepared materials at magnification 50 µm.

TGA previously studied the thermal properties of the chitosan-transition metal compounds under a nitrogen atmosphere**.** In general, it has been found that the coordination of a metal ion with the functional group of the chitosan moiety causes thermal instability and affects thermal degradation. Figure 4 shows TGA diagrams of the prepared chitosan/HBPE/Co relative to the free HBPE and chitosan. The characteristic temperatures and the corresponding mass losses (%) in the prepared composites' main degradation stages are listed in Table 1. It can be noticed that the first peak appeared at 25-128°C explained as resulting from the evaporation of water. The second peak corresponding to the main degradation of chitosan occurred in the temperature range 128-477°C with weight loss (%) about 89.8 % compared to that of the free chitosan HBPE (52 and 49.8 %, respectively). These results indicated the conformation change in chitosan resulted from the mixing of Co metal ions and HBPE and affected the formation of the new phase of the composite, which partly decreased the bond energies of the glycosidic linkages in chitosan, consequently leading to its thermal instability. In other words, the Co metal composite had lower thermal stability than that of chitosan and HBPE. This conclusion is in close agreement with the previous studies [53, 54].

Table 1. TGA data of the prepared composites at different temperatures.

Sample	**Wt loss (%) at different temperatures (°C)**		
	25-128	128-477	> 477
Chitosan	12.2	52	35.8
HBPE	2.8	49.8	47.4
Chitosan/HBPE/Co	66.2	23.6	10.2

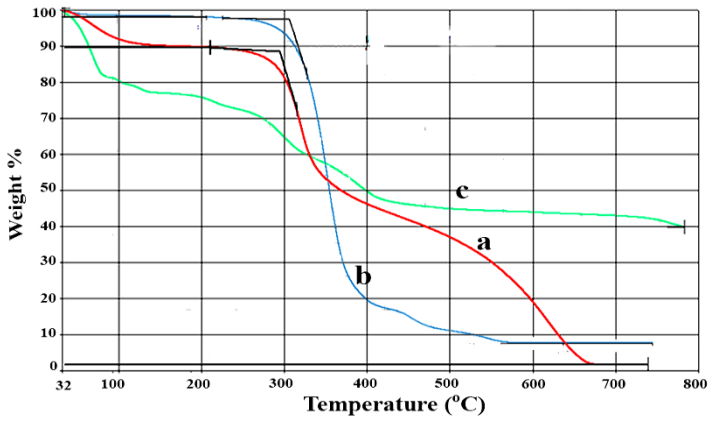

Figure 4. TGA diagrams of chitosan/HBPE/Co composite (c) relative to the free (a) chitosan and (b) HBPE.

3.2. Adsorption studies

3.2.1. Effect of initial dye concentration.

Figure 5a shows the effect of the different concentrations of AB277 dye on the adsorbed percentage of the dye using both chitosan/HBPE/Co and chitosan/HBPE composites at pH 3.0 for a constant time of 1 hour and shaking rate of 400 rpm. The results demonstrated that the rise in dye concentration from 46.59 mg/L to 207.39 mg/L resulted in an increment in dye adsorbed onto chitosan/HBPE chitosan/HBPE/Co composites from 32.1 to 61.3 % and from 85.6 to 94.7 %, respectively. In addition, the adsorption efficiency of chitosan/HBPE/Co composite was higher than that of chitosan/HBPE composite.

3.2.2. Effect of contact time.

Figure 5b shows the effect of contact time on the adsorbed percentage of AB277 dye using both chitosan/HBPE/Co and chitosan/HBPE composites at pH 3.0, an initial dye concentration of about 46.59 mg/L, and 400 rpm. Shaking rate. The effect of dye sorption contact time on the prepared composites was studied for a duration of 15–90 min. With time the percentage of dye sorption gradually decreased from 15 to 90 min. The dye demonstrated rapid adsorption throughout the first 60 min until it reached equilibrium and decreased slowly over time. The quantity of dye removal was greater at the outset because the adsorbent's larger surface area was accessible for the dye's adsorption [55].

3.2.3. Effect of temperature.

Figure 5c shows the effect of temperature on the adsorbed percentage of AB277 dye using both chitosan/HBPE/Co and chitosan/HBPE composites at pH 3.0, an initial dye concentration of about 46.59 mg/L, constant time of 1 h, and shaking rate of 400 rpm.. The result shows that an increase in the temperature, from 25 to 60^{O}C, increased the adsorbed percentage, which refers to the nature of endothermic adsorption.

3.2.4. Effect of sorbent dosage.

Figure 5d shows the effect of sorbent dosage on the adsorbed percentage of AB277 dye using both chitosan/HBPE/Co and chitosan/HBPE composites at pH 3.0, an initial dye concentration of about 46.59 mg/L, constant time 1 h, and shaking rate 400 rpm. The adsorbed

percentage was increased considerably with an increase in the sorbent dosage from 0.03 to 0.12 g. It can conclude that increasing the adsorbent dose at a fixed concentration of AB277 dye provided more adsorption sites available for AB277 dye, thus increasing the dye uptake.

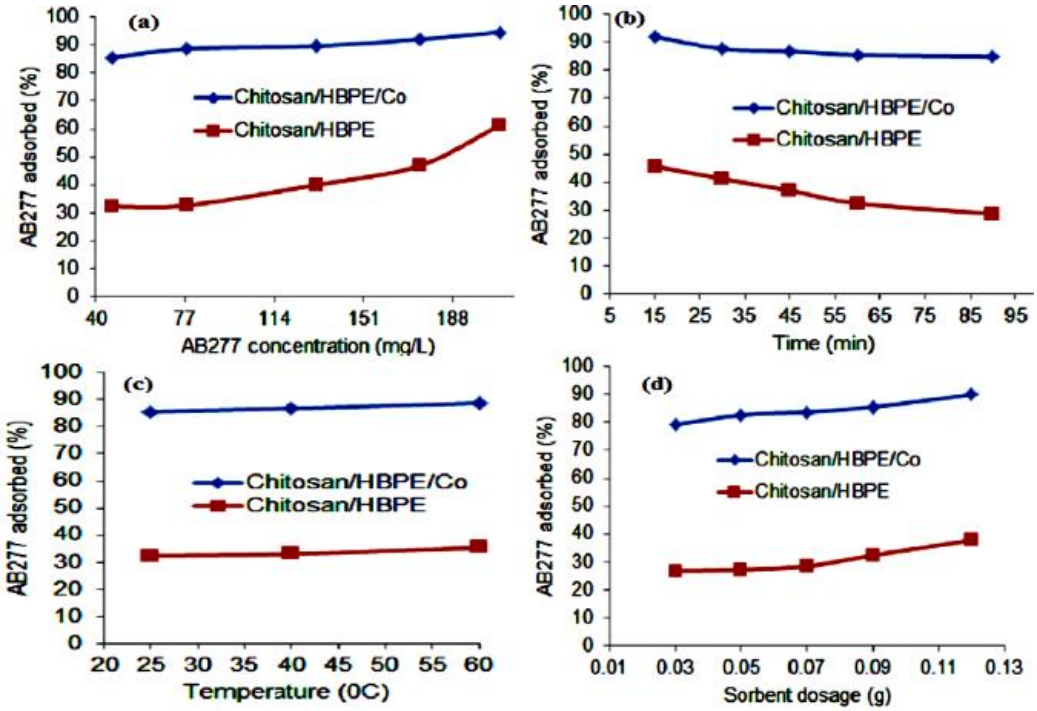

Figure 5. Effect of (a) AB277 dye concentration, (b) time, (c) temperature, and (d) sorbent dosage of the prepared composites at pH 3.0, constant dye concentration 46.59 mg/L, and shaking rate 400 rpm.

3.3. Adsorption isotherm models evaluation.

Isothermic adsorption is necessary to describe the adsorbent-adsorbent interaction. There are numerous models of isotherms used to examine experimental statistics. For this, the isothermic models Langmuir, Freundlich, D–R, and Temkin are examined to match AB277 dye adsorption experimental statistics on chitosan/HBPE/Co and chitosan/HBPE composites [56]. The adsorption isotherms of the prepared composites using different models at an initial dye concentration of 46.59 mg/L. Every model's distinctive isotherm parameters were developed and described in Tables 2 and 3. The linear regression coefficient R^2 (0.9682) obtained from the Langmuir isotherm model is the largest, meaning that the Langmuir isotherm suits very well under the concentration range studied because the active adsorption sites are distributed homogeneously on the chitosan/HBPE/Co. A similar isotherm was obtained in the previous studies [57-59]. The extreme monolayer adsorption capacity (Q_{max}) of the AB277 onto the prepared composites using the Langmuir isotherm model was assessed as 26.74 and 3.19 mg/g. The reciprocal strength factor (n) had values of 1.79 and 2.63 at 25°C for chitosan/HBPE/Co and chitosan/HBPE composites, respectively. Besides, R_L values within the range $0 < R_L < 1$ indicate favorable adsorption and acceptability of the process [60]. Moreover, chitosan/HBPE/Co had a high R_L value (0.49×10^{-3} mg/L) relative to that in the case of chitosan/HBPE composite (4.7×10^{-3} mg/L). Therefore, using chitosan/HBPE/Co composite for AB277 adsorption was more favorable. In addition, the K_F rate has been improved, which represents an exothermic adsorption procedure in nature. The E value significance provides evidence of the adsorption process. If the value of E < 8 kJ/mol is the process controlled by physisorption and in the 8–20 kJ/mol range, the ion-exchange system adsorption is

administered. In other words, the values of E for the present systems were found to be 3.51 and 1.67 kJ/mol for chitosan/HBPE/Co and chitosan/HBPE composites, respectively, which specifies that the physisorption mechanism governs the adsorption of AB277 dye to these adsorbents according to the previous data reported by Fan *et al.* [61]. It is also important to compare the value of Q_{max} obtained from this work with values from other reported modified chitosan and metal-composite adsorbents, as shown in Table 4. The electrostatic interactions are probably needed only to transfer the dye ions to the cationic polymer chitosan's nearest environment. Later, even their mechanical incorporation into composite accompanied by Co-binding dispersion forces seems to be a good reason for dye particles to be attached (Scheme 1).

Table 2. Isotherm constants of AB277 dye adsorption onto chitosan/HBPE/Co composite (under conditions: C_o: 46.59 mg/L, pH 3.0, V: 10 mL and contact time: 1 h, at 25^{O}C).

Isotherm model	Constants (mg/g)			R^2
Langmuir	Q_{max}	R_L (mg/L)		
	26.74	0.49×10^{-3}		0.9682
Freundlich	K_F	n		
	1.53	1.79		0.9326
D-R	Q_s	K_{ad} (mol^2/KJ^2)		
	16.67	0.407		0.9652
Temkin	B (J/mol)	b_T	A_T (L/g)	
	5.31	352.5	3.72	0.8483

Table 3. Isotherm constants of AB277 dye adsorption onto chitosan/HBPE composite (under conditions: C_o: 46.59 mg/L, pH 3.0, V: 10 mL and contact time: 1 h, at 25^{O}C).

Isotherm model	Constants (mg/g)			R^2
Langmuir	Q_{max}	R_L (mg/L)		
	3.19	4.7×10^{-3}		0.8549
Freundlich	K_F	n		
	0.36	2.63		0.6853
D-R	Q_s	K_{ad} (mol^2/KJ^2)		
	2.55	0.179		0.7885
Temkin	B (J/mol)	b_T	A_T (L/g)	
	0.724	2066	5.2	0.6128

Table 4. Comparison of adsorption capacities of dyes on various adsorbents.

Used Materials	Q (mg.g^{-1})	Types of dye	Ref
Chitosan/HBPE/Co	26.74	Acid blue 277	Present work
Chitosan/HBPE	3.19	Acid blue 277	Present work
Chitosan	4.66	Acid blue 158	**[63]**
Chitosan-NaOH	12.3	Direct blue 78	**[64]**
Cu-TiO_2 composites	22.23	Acid blue 80	**[65]**

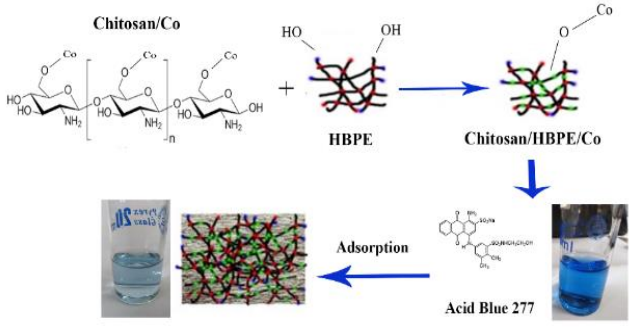

Scheme 1. Schematic diagram outlining the multi-step interaction of AB277 dye with the prepared composite.

The compatibility and adaptation of HBPE macromolecular chains and the dye in such processes are significant. Based on the above considerations, AB277 dye binding by a cationic flocculant in the presence of various anionic substances is a multi-step process [62].

3.4. Adsorption kinetics.

The pseudo-first-order and pseudo-second-order kinetic models were applied to understand the mechanism of the adsorption process. Fig 6 shows the kinetics of AB277 adsorption onto the prepared materials (under conditions: initial dye concentration: 46.59 mg/L, pH 3.0, V: 10 mL, and contact time: 1 h, at 25°C).

Table 5. Kinetic parameters for the adsorption of AB277 dye onto the prepared composites (under conditions: C_o: 46.59 mg/L, pH 3.0, V: 10 mL, and contact time: 1 h, at 25^{O}C).

Composite	Pseudo-first-order kinetic			Pseudo-second-order kinetic		
	K_1	Q_{ecal}	R^2	K_2	Q_{ecal}	R^2
Chitosan/HBPE/Co	0.016	1.15	0.9413	0.017	7.12	0.9971
Chitosan/HBPE	0.004	0.872	0.0764	0.005	0.73	0.4472

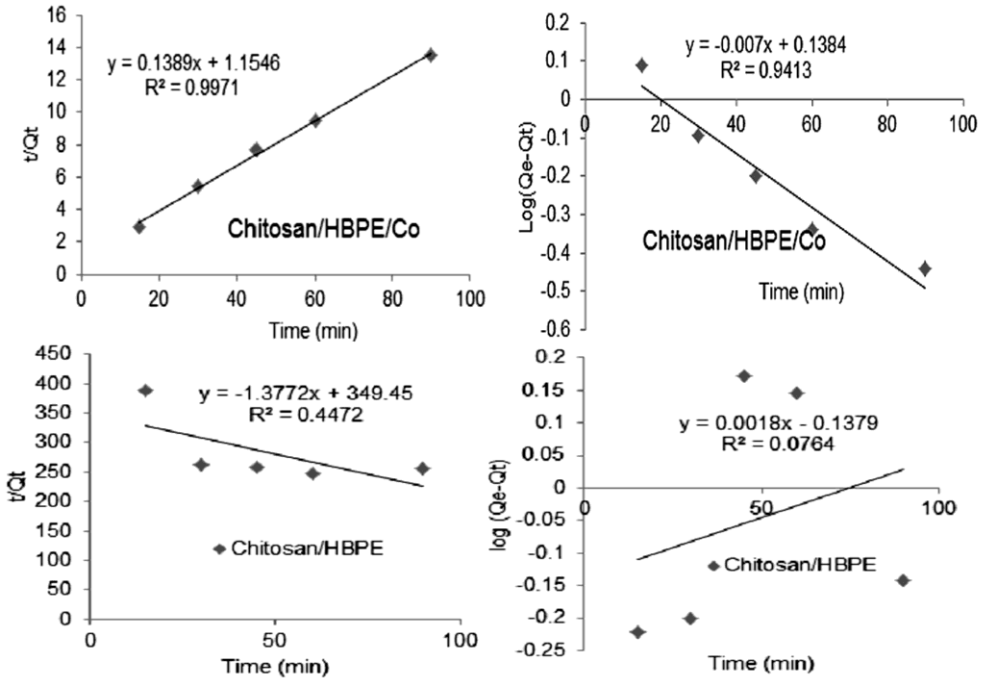

Figure 6. Kinetics of AB277 dye adsorption onto the prepared materials (under condition: C_o: 46.59 mg/L, pH 3.0, V: 10 mL and contact time: 1 h, at 25^{O}C).

In Table 5, the necessary parameters and coefficients of correlation (R^2) acquired from the two kinetic models are given. It can be noted that the pseudo-second-order model R^2 value is greater than that of the pseudo-first-order model and very similar to unity (0.9431 and 0.9971, respectively), indicating the pseudo-second-order model follows the kinetics of AB277 adsorption. The data were added to the intraparticle diffusion model by Weber and Morris [66] to describe the steps that happened during the adsorption process. The Q_t versus plot ($t^{0.5}$) gives two straight intersected segments that do not pass through the origin. These two intersecting segments suggest that adsorption occurs in two steps, with a bulk diffusion followed by intraparticle diffusion, as shown in Figure 7. The divergence from the point of origin suggests that intraparticle diffusion was not the only rate-control stage suggesting several processes regulated the process of dye adsorption [67]. It can therefore be inferred that both the pseudo-second-order and the diffusion of intraparticle took place simultaneously.

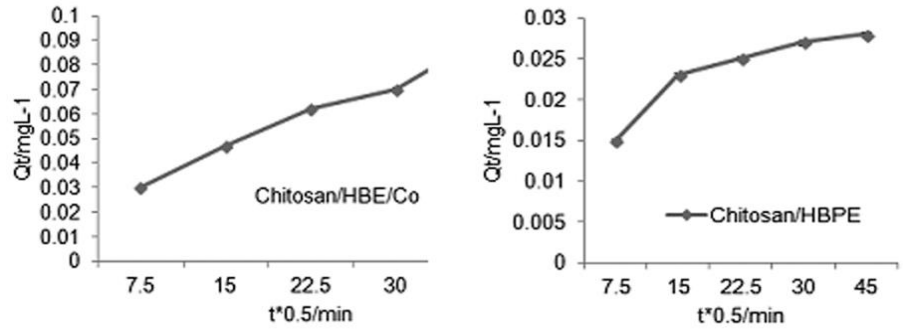

Figure 7. Adsorption of AB277 dye at a different time onto the prepared materials (under the condition: C_o: 46.59 mg/L, pH 3.0, and V: 10 mL at 25^{O}C).

4. Conclusions

This paper reviewed the promising chitosan/HBPE/Co composite's efficiency, prepared by an emulsion strategy for the adsorption of AB277 acid dye from an aqueous medium. The adsorption capacity of AB277 dye was investigated using the different isotherm models (Langmuir, Freundlich, D-R, and Temkin). FTIR, SEM, and TGA revealed that Co metal particles are joined *in situ* on the chitosan/HBPE composite. In addition, the adsorption study demonstrated that the joined of Co metal ions to chitosan/HBPE composite enhanced the adsorbent capacity of AB277 dye. Langmuir isotherm model showed the best conformity compared to the other models. The experimental kinetic data agreed very well to the pseudo-second-order kinetic model.

Funding

The authors disclosed receipt of the following financial support for the research, authorship, and/or publication of this article: This work was supported by the Egyptian Academy of Scientific Research & Technology, Cairo, Egypt (ASRT) (2016/2018).

Acknowledgments

The authors wish to thank The Egyptian Academy of Scientific Research & Technology, Cairo, Egypt (ASRT) for financial supporting of this work according to the Bilateral Joint Project Funding with the Czech Academy of Sciences, Prague, Czech Republic (CAS) 2016/2018.

Conflicts of Interest

The authors declare no conflict of interest.

References

1. Murray, K.E.; Thomas, S.M.; Bodour, A.A. Prioritizing research for trace pollutants and emerging contaminants in the freshwater environment. *Environmental Pollution* **2010**, *158*, 3462-3471, https://doi.org/10.1016/j.envpol.2010.08.009.
2. Richardson, S.D.; Kimura, S.Y. Water Analysis: Emerging Contaminants and Current Issues. *Analytical Chemistry* **2016**, *88*, 546-582, https://doi.org/10.1021/acs.analchem.5b04493.
3. Shannon, M.A.; Bohn, P.W.; Elimelech, M.; Georgiadis, J.G.; Mariñas, B.J.; Mayes, A.M. Science and technology for water purification in the coming decades. *Nature* **2008**, *452*, 301-310, https://doi.org/10.1038/nature06599.
4. Haroun, A.; Mashaly, H.; Helmy, H.; Kamel, M. Kinetic Study of Gelatin/Chitosan Based Nanocomposites for Acid Red 150 Dye Adsorption Using Ultrasonic Energy. *Egyptian Journal of Chemistry* **2017**, *60*, 41-54, https://doi.org/10.21608/EJCHEM.2017.580.1007.

5. Elhalawany, N.; Haroun, A.; Abbas, H.; Hammad, F. Conducting chelating polymer composites based on grafted waste polystyrene for removal of toxic copper ions. *Journal of Elastomers and Plastics* **2013**, *46*, 553-568, https://doi.org/10.1177/0095244313476509.
6. Haroun, A.A.; Mashaly, H.M.; El-Sayed, N.H. Novel nanocomposites based on gelatin/HPET/chitosan with high performance acid red 150 dye adsorption. *Clean Technologies and Environmental Policy* **2013**, *15*, 367-374, https://doi.org/10.1007/s10098-012-0525-y.
7. Haroun, A.A.; El-Halawany, N.R. Preparation and Evaluation of Novel Interpenetrating Polymer Network-Based on Newspaper Pulp for Removal of Copper Ions. *Polymer-Plastics Technology and Engineering* **2011**, *50*, 232-238, https://doi.org/10.1080/03602559.2010.531435.
8. Haroun, A.A.; Taleb, E.M.A.; Abd El-Ghaffar, M.A. Synthesis and Characterization of Novel Thermoplastic Films for Removal of Heavy Metal Ions. *Polymer-Plastics Technology and Engineering* **2010**, *49*, 454-461, https://doi.org/10.1080/03602550903417509.
9. Ahmad, A.; Mohd-Setapar, S.H.; Chuong, C.S.; Khatoon, A.; Wani, W.A.; Kumar, R.; Rafatullah, M. Recent advances in new generation dye removal technologies: novel search for approaches to reprocess wastewater. *RSC Advances* **2015**, *5*, 30801-30818, https://doi.org/10.1039/C4RA16959J.
10. Alsbaiee, A.; Smith, B.J.; Xiao, L.; Ling, Y.; Helbling, D.E.; Dichtel, W.R. Rapid removal of organic micropollutants from water by a porous β-cyclodextrin polymer. *Nature* **2016**, *529*, 190-194, https://doi.org/10.1038/nature16185.
11. Alventosa-deLara, E.; Barredo-Damas, S.; Alcaina-Miranda, M.I.; Iborra-Clar, M.I. Ultrafiltration technology with a ceramic membrane for reactive dye removal: Optimization of membrane performance. *Journal of Hazardous Materials* **2012**, *209-210*, 492-500, https://doi.org/10.1016/j.jhazmat.2012.01.065.
12. Gomez-Maldonado D., Vega Erramuspe I. B., Peresin M. S. Natural polymers as alternative adsorbents and treatment agents for water remediation. *BioRes*. **2019,** *14*, 10093-10160.
13. Bhowmik, K.L.; Deb, K.; Bera, A.; Debnath, A.; Saha, B. Interaction of anionic dyes with polyaniline implanted cellulose: Organic π-conjugated macromolecules in environmental applications. *Journal of Molecular Liquids* **2018**, *261*, 189-198, https://doi.org/10.1016/j.molliq.2018.03.128.
14. Bouyahmed, F.; Cai, M.; Reinert, L.; Duclaux, L.; Dey, R.K.; Youcef, H.B.; Lahcini, M.; Muller, F.; Delpeux-Ouldriane, S.A. Wide adsorption range hybrid material based on chitosan, activated carbon and montmorillonite for water treatment. *C J. Carbon Res.* **2018,** *4*, https://doi.org/10.3390/c4020035.
15. Cova, T.F.; Murtinho, D.; Pais, A.A.C.C.; Valente, A.J.M. Combining Cellulose and Cyclodextrins: Fascinating Designs for Materials and Pharmaceutics. *Frontiers in Chem* **2018,** *6*, https://doi.org/10.3389/fchem.2018.00271.
16. Gautam, D.; Kumari, S.; Ram, B.; Chauhan, G.S.; Chauhan, K. A new hemicellulose-based adsorbent for malachite green. *Journal of Environmental Chemical Engineering* **2018**, *6*, 3889-3897, https://doi.org/10.1016/j.jece.2018.05.029.
17. Jiang, Y.; Liu, B.; Xu, J.; Pan, K.; Hou, H.; Hu, J.; Yang, J. Cross-linked chitosan/β-cyclodextrin composite for selective removal of methyl orange: Adsorption performance and mechanism. *Carbohydrate Polymers* **2018**, *182*, 106-114, https://doi.org/10.1016/j.carbpol.2017.10.097.
18. Li, J.; Zuo, K.; Wu, W.; Xu, Z.; Yi, Y.; Jing, Y.; Dai, H.; Fang, G. Shape memory aerogels from nanocellulose and polyethyleneimine as a novel adsorbent for removal of Cu(II) and Pb(II). *Carbohydrate Polymers* **2018**, *196*, 376-384, https://doi.org/10.1016/j.carbpol.2018.05.015.
19. Morin-Crini, N.; Winterton, P.; Fourmentin, S.; Wilson, L.D.; Fenyvesi, É.; Crini, G. Water-insoluble β-cyclodextrin–epichlorohydrin polymers for removal of pollutants from aqueous solutions by sorption processes using batch studies: A review of inclusion mechanisms. *Progress in Polymer Science* **2018**, *78*, 1-23, https://doi.org/10.1016/j.progpolymsci.2017.07.004.
20. Saad, A.H.A.; Azzam, A.M.; El-Wakeel, S.T.; Mostafa, B.B.; Abd El-latif, M.B. Removal of toxic metal ions from wastewater using ZnO@Chitosan core-shell nanocomposite. *Environmental Nanotechnology, Monitoring & Management* **2018**, *9*, 67-75, https://doi.org/10.1016/j.enmm.2017.12.004.
21. Shao, Z.-J.; Huang, X.-L.; Yang, F.; Zhao, W.-F.; Zhou, X.-Z.; Zhao, C.-S. Engineering sodium alginate-based cross-linked beads with high removal ability of toxic metal ions and cationic dyes. *Carbohydrate Polymers* **2018**, *187*, 85-93, https://doi.org/10.1016/j.carbpol.2018.01.092.
22. Dongre, R.S.; Sadasivuni, K.K.; Deshmukh, K.; Mehta, A.; Basu, S.; Meshram, J.S.; Al-Maadeed, M.A.A.; Karim, A. Natural polymer based composite membranes for water purification: a review. *Polymer-Plastics Technology and Materials* **2019**, *58*, 1295-1310, https://doi.org/10.1080/25740881.2018.1563116.
23. Upadhyay, U.; Sreedhar, I.; Singh, S.A.; Patel, C.M.; Anitha, K.L. Recent advances in heavy metal removal by chitosan based adsorbents. *Carbohydrate Polymers* **2021**, *251*, https://doi.org/10.1016/j.carbpol.2020.117000.
24. Liu, S.; Chen, M.; Cao, X.; Li, G.; Zhang, D.; Li, M.; Meng, N.; Yin, J.; Yan, B. Chromium (VI) removal from water using cetylpyridinium chloride (CPC)-modified montmorillonite. *Separation and Purification Technology* **2020**, *241*, https://doi.org/10.1016/j.seppur.2020.116732.
25. Velasco-Garduño, O.; Martínez, M.E.; Gimeno, M.; Tecante, A.; Beristain-Cardoso, R.; Shirai, K. Copper removal from wastewater by a chitosan-based biodegradable composite. *Environmental Science and Pollution Research* **2020**, *27*, 28527-28535, https://doi.org/10.1007/s11356-019-07560-2.

26. Mohapi, M.; Sefadi, J.S.; Mochane, M.J.; Magagula, S.I.; Lebelo, K. Effect of LDHs and Other Clays on Polymer Composite in Adsorptive Removal of Contaminants: A Review. *Crystals* **2020**, *10*, https://doi.org/10.3390/cryst10110957.
27. Nasir, A.; Masood, F.; Yasin, T.; Hameed, A. Progress in polymeric nanocomposite membranes for wastewater treatment: Preparation, properties and applications. *Journal of Industrial and Engineering Chemistry* **2019**, *79*, 29-40, https://doi.org/10.1016/j.jiec.2019.06.052.
28. Awasthi, A.; Jadhao, P.; Kumari, K. Clay nano-adsorbent: structures, applications and mechanism for water treatment. *SN Applied Sciences* **2019**, *1*, https://doi.org/10.1007/s42452-019-0858-9.
29. Wang, L.; Shi, C.; Wang, L.; Pan, L.; Zhang, X.; Zou, J.-J. Rational design, synthesis, adsorption principles and applications of metal oxide adsorbents: a review. *Nanoscale* **2020**, *12*, 4790-4815, https://doi.org/10.1039/C9NR09274A.
30. Daud, M.; Hai, A.; Banat, F.; Wazir, M.; Habib, M.; Govindan, B.; Al-Harthi, M. A review on the recent advances, challenges and future aspect of layered double hydroxides (LDH) – Containing hybrids as promising adsorbents for dyes removal. *Journal of Molecular Liquids* **2019**, *288*, https://doi.org/10.1016/j.molliq.2019.110989.
31. Xu, G.; Zhu, Y.; Wang, X.; Wang, S.; Cheng, T.; Ping, R.; Cao, J.; Lv, K. Novel chitosan and Laponite based nanocomposite for fast removal of Cd(II), methylene blue and Congo red from aqueous solution. *e-Polymers* **2019**, *19*, 244-256, https://doi.org/10.1515/epoly-2019-0025.
32. Homaeigohar, S. The Nanosized Dye Adsorbents for Water Treatment. *Nanomaterials* **2020**, *10*, https://doi.org/10.3390/nano10020295.
33. Qamar, S.A.; Ashiq, M.; Jahangeer, M.; Riasat, A.; Bilal, M. Chitosan-based hybrid materials as adsorbents for textile dyes—A review. *Case Studies in Chemical and Environmental Engineering* **2020,** https://doi.org/10.1016/j.cscee.2020.100021.
34. Ahmad, M.N.; Hussain, A.; Anjum, M.N.; Hussain, T.; Mujahid, A.; Hammad Khan, M.; Ahmed, T. Synthesis and characterization of a novel chitosan-grafted-polyorthoethylaniline biocomposite and utilization for dye removal from water. *Open Chemistry* **2020**, *18*, 843-849, https://doi.org/10.1515/chem-2020-0137.
35. Nguyen, N.T.; Nguyen, N.T.; Nguyen, V.A. In Situ Synthesis and Characterization of ZnO/Chitosan Nanocomposite as an Adsorbent for Removal of Congo Red from Aqueous Solution. *Advances in Polymer Technology* **2020**, *2020*, https://doi.org/10.1155/2020/3892694.
36. Muinde, V.M.; Onyari, J.M.; Wamalwa, B.; Wabomba, J.N. Adsorption of malachite green dye from aqueous solutions using mesoporous chitosan–zinc oxide composite material. *Environmental Chemistry and Ecotoxicology* **2020**, *2*, 115-125, https://doi.org/10.1016/j.enceco.2020.07.005.
37. Cui, J.; Wang, X.; Yu, S.; Zhong, C.; Wang, N.; Meng, J. Facile fabrication of chitosan-based adsorbents for effective removal of cationic and anionic dyes from aqueous solutions. *International Journal of Biological Macromolecules* **2020**, *165*, 2805-2812, https://doi.org/10.1016/j.ijbiomac.2020.10.161.
38. Wan Ngah, W.S.; Teong, L.C.; Hanafiah, M.A.K.M. Adsorption of dyes and heavy metal ions by chitosan composites: A review. *Carbohydrate Polymers* **2011**, *83*, 1446-1456, https://doi.org/10.1016/j.carbpol.2010.11.004.
39. Kim S.K. *Chitin, Chitosan, Oligosaccharides and Their Derivatives: Biological Activities and Applications.* CRC Press, New York, USA, **2010**.
40. Almeida, F.T.R.d.; Ferreira, B.C.S.; Moreira, A.L.d.S.L.; Freitas, R.P.d.; Gil, L.F.; Gurgel, L.V.A. Application of a new bifunctionalized chitosan derivative with zwitterionic characteristics for the adsorption of Cu2+, Co2+, Ni2+, and oxyanions of Cr6+ from aqueous solutions: Kinetic and equilibrium aspects. *Journal of Colloid and Interface Science* **2016**, *466*, 297-309, https://doi.org/10.1016/j.jcis.2015.12.037.
41. Azlan, K.; Wan Saime, W.N.; Lai Ken, L. Chitosan and chemically modified chitosan beads for acid dyes sorption. *Journal of Environmental Sciences* **2009**, *21*, 296-302, https://doi.org/10.1016/S1001-0742(08)62267-6.
42. Chen, X. Modeling of Experimental Adsorption Isotherm Data. *Information* **2015,** *6*, *14-22*. https://doi.org/10.3390/info6010014.
43. Langmuir, I. The Constitution And Fundamental Properties Of Solids And Liquids. Part I. Solids. *Journal of the American Chemical Society* **1916**, *38*, 2221-2295, https://doi.org/10.1021/ja02268a002.
44. Frundlich H.M.F. Over the adsorption in solution. *J. Phys. Chem.* **1906,** *57*, 385-471.
45. Dubinin, M.M.; Radushkevich, L.V**.** The equation of the characteristic curve of the activated charcoal. *Proc. Acad, Sci. USSR Phys. Chem. Sect.* **1947,** *55*, 331-337.
46. Temkin, M.I.; Pyzhev, V. Kinetics of ammonia synthesis on promoted iron catalyst. *Acta Physiochem. URSS* **1940,** *12*, 217-222.
47. Haroun, A.A.; Hakeim, O.A.; Trhlíková, O.; Šlouf, M.; Netopilík, M. Preparation and characterization of metal complex hydrogels crosslinked with hyperbranched polyester. *Egypt. J. Chem.* **2017,** *60*, 849-856, https://doi.org/10.21608/EJCHEM.2017.1310.1081.
48. A.O, D.; Olalekan, A.; Olatunya, A.; Dada, A.O. Langmuir, Freundlich, Temkin and Dubinin–Radushkevich Isotherms Studies of Equilibrium Sorption of Zn 2+ Unto Phosphoric Acid Modified Rice Husk. *J. Appl. Chem.* **2012**, *3*, 38-45, https://doi.org/10.9790/5736-0313845.

49. Ahmad, A.; Razali, M.H.; Mamat, M.; Mehamod, F.S.B.; Anuar Mat Amin, K. Adsorption of methyl orange by synthesized and functionalized-CNTs with 3-aminopropyltriethoxysilane loaded TiO2 nanocomposites. *Chemosphere* **2017**, *168*, 474-482, https://doi.org/10.1016/j.chemosphere.2016.11.028.
50. Daniel Thangadurai, T.; Ihm, S.K. Chiral Schiff Base Ruthenium(II) Carbonyl Complexes: Synthesis, Characterization, Catalytic and Antibacterial Studies. *Synthesis and Reactivity in Inorganic, Metal-Organic, and Nano-Metal Chemistry* **2006**, *36*, 435-440, https://doi.org/10.1080/15533170600732767.
51. Antony, R.; Theodore David, S.; Saravanan, K.; Karuppasamy, K.; Balakumar, S. Synthesis, spectrochemical characterisation and catalytic activity of transition metal complexes derived from Schiff base modified chitosan. *Spectrochimica Acta Part A: Molecular and Biomolecular Spectroscopy* **2013**, *103*, 423-430, https://doi.org/10.1016/j.saa.2012.09.101.
52. Trimukhe, K.D.; Varma, A.J. Metal complexes of crosslinked chitosans: Correlations between metal ion complexation values and thermal properties. *Carbohydrate Polymers* **2009**, *75*, 63-70, https://doi.org/10.1016/j.carbpol.2008.06.011.
53. Sreenivasan, K. Thermal stability studies of some chitosanmetal ion complexes using differential scanning calorimetry. *Polymer Degradation and Stability* **1996**, *52*, 85-87, https://doi.org/10.1016/0141-3910(95)00220-0.
54. Ou, C.-Y.; Li, S.-D.; Li, C.-P.; Zhang, C.-H.; Yang, L.; Chen, C.-P. Effect of cupric ion on thermal degradation of chitosan. *Journal of Applied Polymer Science* **2008**, *109*, 957-962, https://doi.org/10.1002/app.28001.
55. Wong, Y.C.; Szeto, Y.S.; Cheung, W.H.; McKay, G. Adsorption of acid dyes on chitosan—equilibrium isotherm analyses. *Process Biochemistry* **2004**, *39*, 695-704, https://doi.10.1016/S0032-9592(03)00152-3.
56. Elsherbiny, A.S.; Salem, M.A.; Ismail, A.A. Influence of the alkyl chain length of cyanine dyes on their adsorption by Na+-montmorillonite from aqueous solutions. *Chemical Engineering Journal* **2012**, *200-202*, 283-290, https://doi.org/10.1016/j.cej.2012.06.050.
57. Annadurai, G.; Ling, L.Y.; Lee, J.-F. Adsorption of reactive dye from an aqueous solution by chitosan: isotherm, kinetic and thermodynamic analysis. *Journal of Hazardous Materials* **2008**, *152*, 337-346, https://doi.org/10.1016/j.jhazmat.2007.07.002.
58. Cheung, W.H.; Szeto, Y.S.; McKay, G. Intraparticle diffusion processes during acid dye adsorption onto chitosan. *Bioresource Technology* **2007**, *98*, 2897-2904, https://doi.org/10.1016/j.biortech.2006.09.045.
59. Azlan, K.; Wan Saime, W.N.; Lai Ken, L. Chitosan and chemically modified chitosan beads for acid dyes sorption. *Journal of Environmental Sciences* **2009**, *21*, 296-302, https://doi.org/10.1016/S1001-0742(08)62267-6.
60. Das, S.K.; Bhowal, J.; Das, A.R.; Guha, A.K. Adsorption Behavior of Rhodamine B on Rhizopus oryzae Biomass. *Langmuir* **2006**, *22*, 7265-7272, https://doi.org/10.1021/la0526378.
61. Fan, H.; Zhou, L.; Jiang, X.; Huang, Q.; Lang, W. Adsorption of Cu2+ and methylene blue on dodecyl sulfobetaine surfactant-modified montmorillonite. *Applied Clay Science* **2014**, *95*, 150-158, https://doi.org/10.1016/j.clay.2014.04.001.
62. Zemaitaitiene, R.J.; Zliobaite, E.; Klimaviciute, R.; Zemaitaitis, A. The role of anionic substances in removal of textile dyes from solutions using cationic flocculant. *Colloids and Surfaces A: Physicochemical and Engineering Aspects* **2003**, *214*, 37-47, https://doi.org/10.1016/S0927-7757(02)00406-5.
63. Kalaivani, G.; Sowmya, A.; Meenakshi, S. Removal of reactive red 2 and acid blue 158 onto chitin/chitosan. *Indian Journal of Environmental Protection* **2011**, *31*, 292-300.
64. Murcia-Salvador, A.; Pellicer, J.A.; Fortea, M.I.; Gómez-López, V.M.; Rodríguez-López, M.I.; Núñez-Delicado, E.; Gabaldón, J.A. Adsorption of Direct Blue 78 Using Chitosan and Cyclodextrins as Adsorbents. *Polymers* **2019**, *11*, 1003-1021, https://doi.org/10.3390/polym11061003.
65. Puentes-Cárdenas, I.J.; Chávez-Camarillo, G.M.; Flores-Ortiz, C.M.; Cristiani-Urbina, M.d.C.; Netzahuatl-Muñoz, A.R.; Salcedo-Reyes, J.C.; Pedroza-Rodríguez, A.M.; Cristiani-Urbina, E. Adsorptive Removal of Acid Blue 80 Dye from Aqueous Solutions by Cu-TiO2. *J. Nanomaterials* **2016,** *2016*, https://doi.org/10.1155/2016/3542359.
66. Weber, W.J.; Morris, J.C**.** Kinetics of Adsorption on Carbon from Solutions. *J. Sanitary Eng. Div* **1963,** *89*, 31-60.
67. Elsherbiny, A.S.; El-Hefnawy, M.E.; Gemeay, A.H. Linker impact on the adsorption capacity of polyaspartate/montmorillonite composites towards methyl blue removal. *Chemical Engineering Journal* **2017**, *315*, 142-151, https://doi.org/10.1016/j.cej.2017.01.002.